Nano Energy 88 (2021) 106205

Contents lists available at ScienceDirect

Nano Energy

journal homepage: www.elsevier.com/locate/nanoen

PEO based polymer in plastic crystal electrolytes for room temperature high-voltage lithium metal batteries

Yulong Liu [a,*], Yang Zhao [b], Wei Lu [a], Liqun Sun [a], Lin Lin [a], Matthew Zheng [b], Xueliang Sun [b,*], Haiming Xie [a,*]

[a] National & Local United Engineering Laboratory for Power Battery, Department of Chemistry, Northeast Normal University, Changchun 130024, China
[b] Department of Mechanical and Materials Engineering, University of Western Ontario, London, Ontario N6A 5B9, Canada

ARTICLE INFO

Keywords:
PEO
Plastic crystal
Lithium metal
High voltage
Interface

ABSTRACT

Lithium metal coupled with high voltage cathodes has been extensively investigated to meet the demand for higher energy density batteries. However, only a few electrolytes are compatible with both lithium anode and high voltage $LiNi_{0.5}Mn_{0.3}Co_{0.2}O_2$. Pure poly(ethylene oxide) electrolyte shows high-stability against lithium metal but has limited oxidation stability (typically < 3.8 V). Nitrile-based electrolyte with -C≡N groups exhibits excellent electrochemical stability against high voltage electrodes. Here, a novel type of poly(ethylene oxide) based polymer in plastic crystal (succinonitrile) electrolyte is designed to achieve stable cathode/electrolyte and anode/electrolyte interfaces simultaneously through strong intermolecular interactions. Li-Li symmetric cells with the polymer in plastic crystal electrolyte runs stably for 700 h at 1 mA cm^{-2}. Even with a high cut-off voltage of 4.4 V, the Li// $LiNi_{0.5}Mn_{0.3}Co_{0.2}O_2$ cell delivers a high discharge capacity of 169 mA h g^{-1} and a capacity retention of 80% after 120 cycles. Our work highlights development of PEO-based electrolytes with higher energy density by inter-molecular design.

1. Introduction

With the growing interest in developing higher energy density batteries, solid-state batteries with a Li metal anode have attracted great attention during recent years [1]. Currently, Bluecar in France has commercialized with a Li/solid polymer electrolyte/$LiFePO_4$ chemistry [2]. The solid polymer electrolyte used is poly(ethylene oxide) (PEO) electrolyte, which demonstrates high safety due to elimination of flammable solvent while possessing excellent flexibility [3]. Commercialized PEO electrolyte is only compatible with 3.6 V $LiFePO_4$ cathode, resulting in an energy density of 250 W h kg^{-1} at most, which prevents these batteries from meeting the increasing demand for long-range EVs. However, high voltage layered structured cathodes (such as $LiCoO_2$, $LiNi_{0.5}Mn_{0.3}Co_{0.2}O_2$) for PEO-based SSBs experience notable capacity decay during cycling [4,5]. The reason for the capacity decay is related to the strong oxidation capability of transition metal ions at the high valence state [6]. As reported by Li et al., pure PEO decomposed at a cut-off voltage of 4.5 V. With $LiCoO_2$ as the cathode, the decomposition voltage decreases to 4.2 V due to the strong oxidative phase of de-lithiated $Li_{1-x}CoO_2$ [7]. To overcome this problem, two strategies have been adopted including cathode interface engineering and use of interlayers. Coating layers such as Al_2O_3 and lithium ion conductors ($Li_{1+x}Al_xTi_{2-x}(PO_4)_3$) have been shown to prevent the direct contact of PEO and the high voltage cathode, thus limiting the side reaction [7–9]. Interlayers have been introduced to construct a stable cathode electrolyte interface (CEI) layer on the cathode, which have been effectively demonstrated in elongating the lifetime of a solid polymer battery [10–12].

Marchiori et al. investigated the electrochemical window of PEO polymer by density functional calculation (DFT). The result indicated that the theoretical oxidation voltage of PEO is 3.65 V [13]. To extend the electrochemical window of PEO electrolyte, sandwich structure electrolytes [14–16], composite electrolytes [17–20], and co-polymer electrolytes [21–23], were proposed in previous reports [24,25]. However, the modified PEO electrolyte still showed limited stability against high voltage electrolyte in long term cycling. Recently, Wu et al. reported a new type of polymer in the ionic liquid system ($Li(DME)_{0.7}$F-SI-$PEO_{0.6}$). This electrolyte was proven to be stable up to 4.5 V due to the donation of lone electron pairs of ether oxygen atoms (from DME and PEO) to Li cations [26]. Succinonitrile based plastic crystal electrolyte

* Corresponding authors.
E-mail addresses: liuyl290@nenu.edu.cn (Y. Liu), xsun9@uwo.ca (X. Sun), xiehm136@nenu.edu.cn (H. Xie).

https://doi.org/10.1016/j.nanoen.2021.106205
Received 27 April 2021; Received in revised form 24 May 2021; Accepted 25 May 2021
Available online 4 June 2021

(PCE) have been widely investigated for its high ionic conductivity and high voltage stability [27]. In addition, SN based PCE showed negligible vapor pressure and low flammability, indicating high safety properties in lithium ion batteries. However, it is unstable against Li metal due to the side reactions, namely, polymerization of nitriles catalyzed by lithium metal [28,29].

In this work, we propose a new concept of polymer in plastic crystal electrolyte (PIPCE) to fabricate PEO-based electrolytes through mixing PEO with the succinonitrile-based plastic crystal (LiTFSI-$SN_{0.05}$-x wt.% FEC, X = 0, 10, 20%). The PIPCE electrolyte of (LiTFSI-$SN_{0.05}$-10 wt.% FEC)−15 wt. %PEO shows an electrochemical oxidation potential up to 4.97 V vs Li/Li^+, almost 1.5 V higher than that of pure PEO. A stable Li metal plating/stripping in Li-Li symmetric cell is achieved for 700 h with a plating capacity of 1 mAh at room temperature (30 °C). The full cell using $LiNi_{0.5}Mn_{0.3}Co_{0.2}O_2$ (NMC532) as cathode can be stably cycled with this electrolyte for 120 cycles under a high charge cutoff voltage of 4.4 V. Such a superior performance can be traced to the strong intermolecular interaction of polymer and salt, which results in stable electrode/electrolyte interfaces as revealed by microstructural analysis.

2. Results

A series of polymers in plastic crystal electrolyte (PIPCE) were prepared by mixing PEO polymer with PCE electrolyte. Later on, the PIPCE electrolyte was loaded onto the PE separator for battery assembly, with a thickness of 22 μm (Fig. S1). The ionic conductivities of different PIPCE were measured by impedance spectroscopy using stainless steel as a blocking electrode, and PIPCE was immersed in Glass Fiber for convenience. Room temperature (30 °C) conductivities for 5% PEO PIPCE, 15% PEO PIPCE and 25% PEO PIPCE are ~3.1×10^{-4} S cm^{-1}, 1.0×10^{-4} S cm^{-1}, and 0.9×10^{-4} S cm^{-1}, respectively (Fig. 1a). For pure PEO electrolyte, the ionic conductivity is measured to be about 8×10^{-6} S cm^{-1} at room temperature (Fig. S2). Conductivity of PIPCE is higher than nano-SiO_2/PEO electrolyte in the temperature range of 30–60 °C as well [20]. PEO dissolved in SN will increase the viscosity of the PCE electrolyte and decrease the lithium ion mobility (Fig. S3). Temperature dependence of ionic conductivity for three PIPCEs were measured between 4 and 60 °C, as shown in Fig. 1b. The Vogel-Tammann-Fulcher empirical formula was used to fit the profiles (Fig. S4). Activation energy of PIPCE is 13.84 kJ mol^{-1}, 10.39, and 3.90 kJ mol^{-1} respectively for 5% PEO PIPCE, 15% PEO PIPCE, and 25% PEO PIPCE. The oxidation stability of PIPCEs was also investigated by linear sweep voltammetry (LSV). As shown in Fig. 1**c**, the oxidation phenomenon starts at 4.73 V for 5% PEO based PIPCE. With increasing content of PEO, the oxidation voltage is increased to 4.97 V (15% PEO and 25% PEO based PIPCE), 1.47 V higher than that of pure PEO (3.5 V). The transference number of lithium ion was obtained with potentiostatic polarization test and electrochemical impedance measurement. Higher lithium transference number denotes the reduced anion movement and reducing ion concentration gradients, resulting in better Li metal anode stability. The lithium transference number (t_{Li}^+) of 5% PEO PIPCE, 15% PEO PIPCE, and 25% PEO PIPCE are 0.48, 0.31, and 0.24, respectively (Figs. 1d and S5). The number is higher than that of pure PEO solid polymer electrolyte (0.19).

To better understand the high oxidation properties of PIPCEs, FTIR and Raman spectra of PIPCEs were measured. According to the FTIR

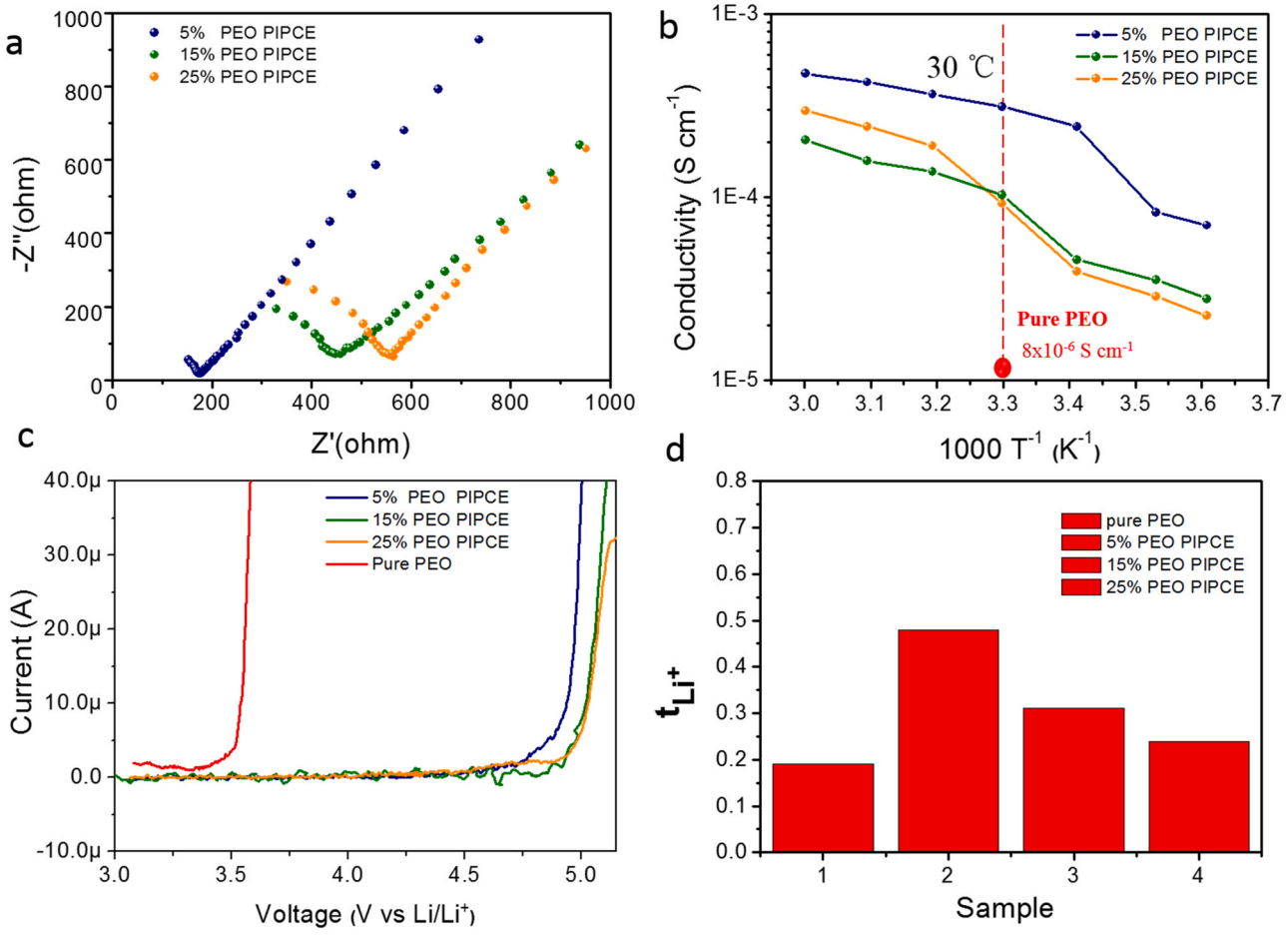

Fig. 1. Electrochemical performance of prepared PIPCEs. (a) Impedance of PIPCE electrolytes at 30 °C (b) Temperature dependence of the ionic conductivity for PIPCEs and PEO (g) LSV curves of PIPCE electrolytes and PEO. (h) Lithium ion transference number of PIPCE electrolytes and PEO.

results in Fig. 2a, two peaks at ~2254 cm^{-1} and ~2275 cm^{-1} are assigned to free SN and Li coordinated-SN, respectively [30]. With an increasing amount of PEO, SN interaction with Li is decreased due to the redshift of free SN peak from ~2254 cm^{-1} to 2252 cm^{-1}. Furthermore, a Li-(C-O-C) peak at 1300 cm^{-1} emerges, which indicates that PEO interacts with Li-ion [31]. In addition, PEO coordination with Li-ion is further demonstrated by the peaks that appeared at ~1080 cm^{-1} (Fig. S6), similar to the reported PEO polymer electrolyte [32,33]. From the Raman spectra in the region of 730–760 cm^{-1} in Fig. 2b, the peak ascribed to free $TFSI^-$ is depressed with increasing content of PEO. This means that the TFSI anion interaction with Li cation is enhanced and anti-oxidation capability is increased [26]. Therefore, Li-ion was observed to interact with the SN molecule, PEO molecule, and TFSI anion, simultaneously. Thus, the reduction of free SN on Li metal and oxidation of PEO on NMC surface is hampered due to these strong intermolecular interactions. Phase content is identified with X-ray diffraction (Fig. 2c), only two diffraction peaks of SN are observed in PIPCE [34]. Diffraction peaks of PEO at 18.9° and 23.1° are undetected, indicating that PEO is in an amorphous state. No LiTFSI salt peaks are observed due to the full dissociation of lithium salt in the PIPCE. Thermal properties of the PIPCE was evaluated by thermogravimetric analysis, as shown in Fig. 2d. The PIPCE is thermally stable over 150 °C, and SN is decomposed at 230 °C [35]. In addition, flammability tests were performed on PIPCEs using a lighter at room temperature (Video S1-S3). All three PIPCEs do not catch fire, which indicates high safety for practical application.

Supplementary material related to this article can be found online at doi:10.1016/j.nanoen.2021.106205.

Supplementary material related to this article can be found online at doi:10.1016/j.nanoen.2021.106205.

Supplementary material related to this article can be found online at doi:10.1016/j.nanoen.2021.106205.

To evaluate the anode stability of PIPCE against Li metal, symmetrical cells were assembled and tested with different capacities. For 5% PEO based PIPCE, as illustrated in Fig. 3a, the voltage profiles were unstable at a current density of 0.5 mA cm^{-2}. The overpotential increased drastically due to the polymerization of nitrile at the Li metal surface. After a 550 h test, the overpotential rised up to 1 V and dropped down due to the formation of soft dendrites. The 15% PEO and 25 PEO PIPCEs were tested at 0.05 mA cm^{-2}, 0.1 mA cm^{-2}, and 0.2 mA cm^{-2}. The overpotential of 15% PEO PIPCE against Li metal is 8 mV, 16 mV, and 32 mV at each respective current densities (Fig. 3b). For 25% PEO PIPCE, the overpotential was measured to be 5 mV, 10 mV, and 20 mV (Fig. S7). Because of the stability of PIPCE at a low current density for 400 h without short-circuiting, the current density was increased to 1 mA cm^{-2}. As presented in Fig. 3c, the overpotential of 25% PEO PIPCE drastically increased to 250 mV while the overpotential of 15% PEO PIPCE was still 100 mV (Fig. 3d and e). Moreover, the cell with 25% PEO PIPCE was short-circuited at 244 h. This could be traced to the low lithium ion conductivity and low lithium transference number of this electrolyte. The lithium dendrite formation is easy at the Li metal surface under this condition. Even after a 700 h test, the Li//Li symmetrical cell with 15% PEO PIPCE still showed negligible overpotential change, suggesting good compatibility against Li metal.

Li metal batteries with NMC 532 cathodes were cycled with a 4.2 and 4.4 V cutoff voltage. The cycling performance of PIPCE was first investigated under the voltage window of 2.7–4.2 V at a C-rate of 0.1 C, as shown in Fig. 4a. Li-NMC 532 cell with 5%, 15% and 25% PEO PIPCE delivered discharge capacities of 154, 140, and 101 mAh g^{-1} and initial coulombic efficiencies (CE) of 84.7%, 76.32%, and 76.85%,

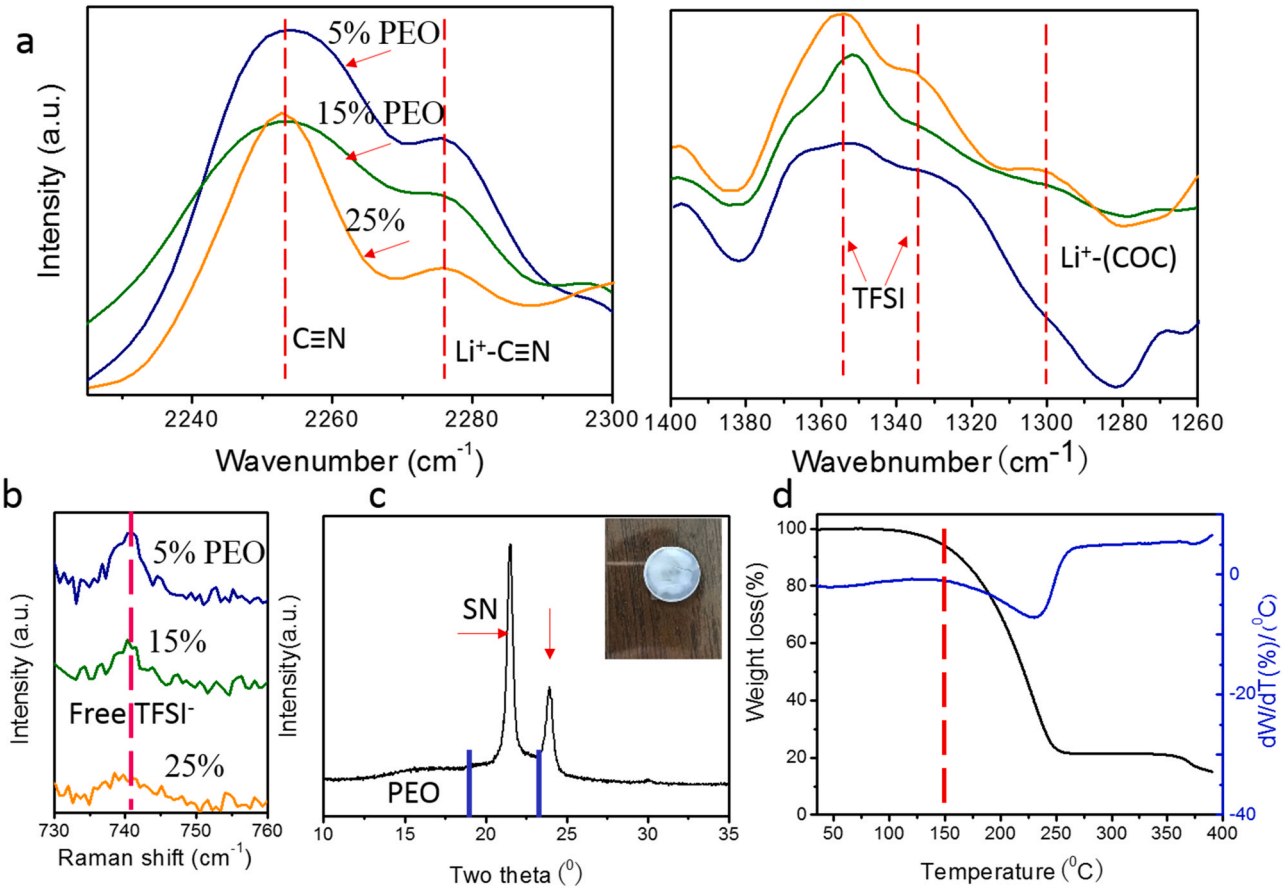

Fig. 2. Physical performance of prepared PIPCEs. (a) FTIR spectra of PIPCE electrolytes in the range of 2225–2300 cm^{-1} and 1200–1400 cm^{-1}. (b) Raman spectra of PIPCE electrolytes in the range of 730–750 cm^{-1} (c) XRD patterns and (d) TG curves of PIPCE electrolyte.

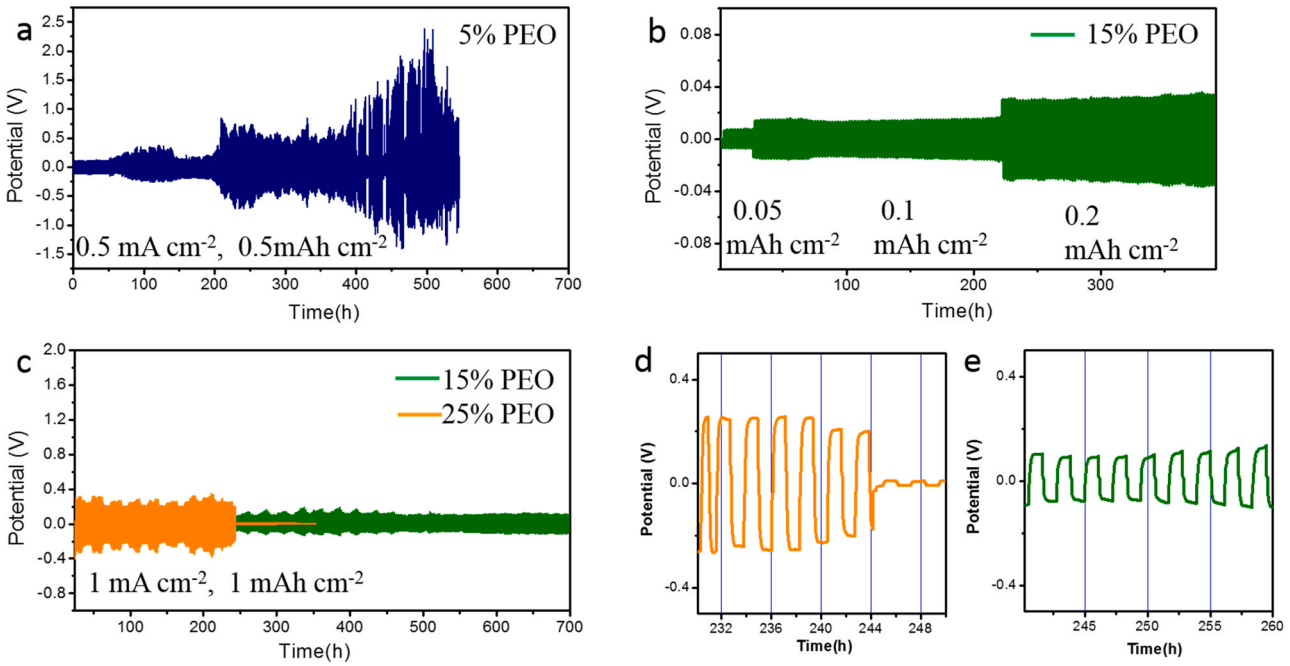

Fig. 3. Voltage profiles of Li metal plating/stripping in Li//Li cells (a) 5% PEO PIPCE under a current density of 0.5 mA cm^{-2} and an areal capacity of 0.5 mA h cm^{-2}. (b) 15% PEO PIPCE under a current density of 0.05, 0.1, and 0.2 mA cm^{-2}. (c) 15% PEO and 25% PEO PIPCE under a current density of 1 mA cm^{-2} and an areal capacity of 1 mA h cm^{-2} and (d, e) Enlarged view of (c).

respectively. This behavior is in accordance with the ionic conductivity of each electrolyte. After 40 cycles, the capacity retention rate of 15% PEO PIPCE was 100% and the average CE was close to 100%. The cell with 5% PEO PIPCE showed a discharge capacity of 136 mA h g^{-1} after 30 cycles, with a capacity loss of 11%. The 1st, 10th, and 40th charge and discharge profiles are well overlapped, as illustrated in Fig. 4b. The overpotential of the cell was small and did not change with cycling, suggesting high cathode stability. In addition, different ratios of fluoroethylene carbonate (FEC) additive were evaluated with NMC cathodes in the voltage window of 2.7–4.2 V. PIPCE without FEC showed a quick decay during cycling, the initial capacity of 139 mA h g^{-1} dropped to 75 mA h g^{-1} after 40 cycles (Fig. S8). With 10 wt% FEC, the stability is greatly enhanced and capacity was kept at 150 mA h g^{-1} during cycling. Although the pure PCE electrolyte delivered a high reversible capacity (150 mA h g^{-1}), the capacity decreased to 110 mA h g^{-1} after 100 cycles (Fig. S9).

When the cutoff voltage was increased to 4.4 V, 15% PEO PIPCE showed the highest capacity of 169 mA h g^{-1} and maintained a capacity retention of 80% after 120 cycles (134 mA h g^{-1} was obtained) (Fig. 4c). The 1st, 10th and 100th charge and discharge profiles are presented in Fig. 3d. The overpotential of the cell slightly increased after 10 cycles and was kept at this level for the following cycles. 25% PEO PIPCE showed a capacity of 101 mA h g^{-1} and capacity retention of 72% for 120 cycles. The capacity loss of 5% PEO PIPCE was 40% and only 92 mA h g^{-1} was obtained after 120 cycles. In comparison, the capacity of NMC in pure PCE decreased from an initial 150 mA h g^{-1} to 73 mA h g^{-1} (50% capacity was retained) at 120 cycles, due to the side reactions at the anode side. To understand the interface stability during charge-discharge, the impedances of Li/PIPCE/NMC were recorded after cycling. As illustrated in Fig. S10, R_0 in equivalent circuit represents the contribution from PIPCE, R_1 is the interfacial resistance of Li/PIPCE and R_2 is the interfacial resistance of PIPCE/NMC 532 [36]. The interfacial resistance of Li/PIPCE is stable, indicating good stability at Li side. The interfacial resistance between PIPCE/NMC is changed from 50 ohm to 232 ohm with a 4.2 V cutoff voltage, and to 318 ohm with a 4.4 V (Table S2).

Due to the high stability, 15% PEO PIPCE was chosen for rate performance testing with a voltage window of 2.7–4.2 V (Fig. 4e). The cell demonstrated a charge capacity of 0.5 mA h cm^{-2} (130 mA h g^{-1}) and retained a charge capacity of 0.487 mA h cm^{-2} (126 mA h g^{-1}) after 100 cycles, corresponding to a capacity retention of 97.4%. Additionally, the cell showed a capacity of 0.4 mA h cm^{-2} (105 mA h g^{-1}) and 0.3 mA h cm^{-2} (80 mA h g^{-1}) at a current rate of 0.2 C and 0.4 C. As the current is changed back to 0.1 C, the charge capacity goes back to 0.46 mA h cm^{-2} (118 mA h g^{-1}). Such a rate performance is better than most reported PEO based solid polymer electrolytes [37–39]. PIPCE is also superior to Ca-CeO_2/PEO composite electrolyte in terms of oxidation voltage and charge capacity [40].

To understand the oxidation stability of 15% PEO-based PIPCE against an NMC cathode, X-ray Photoelectron Spectroscopy (XPS) analysis was performed on cycled cells. As presented in Fig. 5a, the C 1s spectra after cycling can be deconvolved into three peaks at 284.1, 286.3, and 292 eV, which can be assigned to the C–C, C–O/C≡N, and C–F bond. The C-O/C≡N peak is attributed to PEO and SN decomposition in the formation of cathode electrolyte interphase on NMC [41]. Three peaks at 397.1, 398.5, and 399.5 eV of N 1s spectra can be assigned to N rich compounds, C═N–C and C≡N bond, respectively. The formation of C═N-C and N rich compound indicates the polymerization of nitrile groups on NMC cathode under a 4.2 V cutoff voltage [42]. The S 2p spectra at 168.7 eV and 169.8 eV (doublet) indicate the presence of SO_2F species at the NMC surface, which is the result of $TFSI^-$ decomposition at high voltage. No oxidation phase such as sulfate is observed, indicating good phase stability of NMC at high voltage [26]. Three peaks at 684.6 eV, 687.2 eV, and 688.4 eV can be observed in the F 1s spectrum. The LiF content in NMC with a 4.4 V cutoff voltage is higher than that cycled with a 4.2 V cutoff voltage. High content of LiF at the surface is beneficial for suppressing decomposition of SN and PEO molecules at high voltage [43].

To further analyze the structure evolution of NMC cathode after cycling, scanning electron microscopy (SEM) and transmission electron microscopy (TEM) were performed. After 100 cycles, SEM images of the NMC under 4.2 V and 4.4 V showed that the NMC particles were covered by thin films without obvious damage (Fig. 5a). With selected area electron diffraction pattern (SAED), it was observed that the R-3m

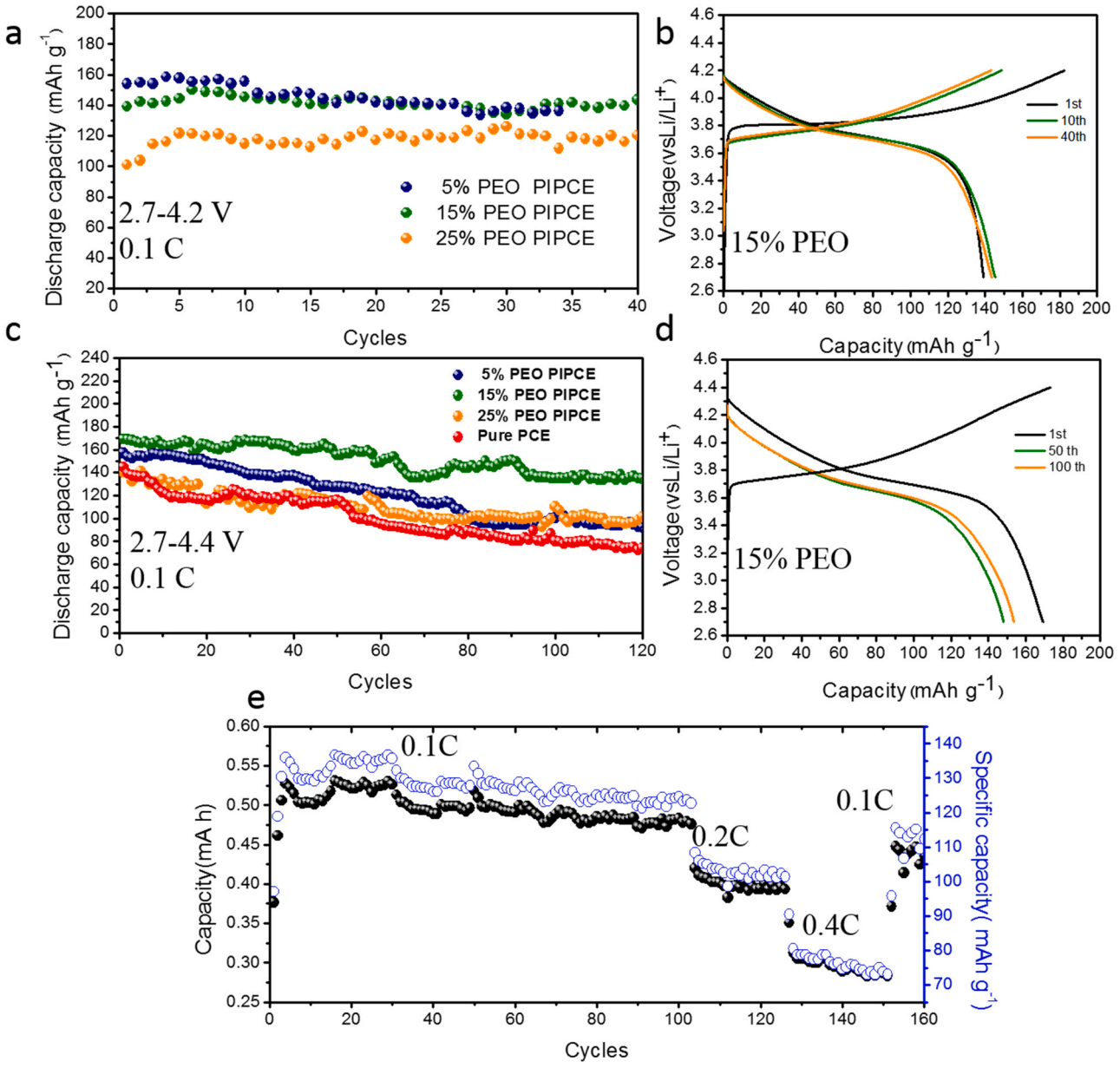

Fig. 4. Long term cycling performance of in Li//NMC 532 cells (a, c) at a cutoff voltage of 4.2 V and 4.4 V for PIPCEs. (b, d) Charge discharge profile of Li//NMC 532 cells with 15% PEO PIPCE at different cut-off voltages. (e) Rate performance of Li//NMC 532 cells with 15% PEO PIPCE.

crystal structure of NMC remains as pristine after charging to 4.2 V and 4.4 V (Fig. 5b). Even at 4.4 V, no crack is observed from TEM images, indicating good compatibility between the PIPEC electrolyte and the NMC cathode. From the high-resolution transmission electron microscopy (HRTEM) images in Fig. 5b, CEI layers are observed for NMC when charged to 4.2 V and 4.4 V. The thickness of CEI is 4.4 nm and 8 nm, respectively. The CEI film can effectively suppress the phase transition of NMC at high voltage [43]. To detect the surface structure information, the lattice fringes of NMC charged to 4.2 V and 4.4 V were analyzed. In both samples, the surface lattice can be assigned to the (104) crystal plane of R-3m (Fig. 5b), suggesting surface stability of NMC in PIPCE electrolyte.

In addition to ensuring a stable cathode interface, the Li anode interface also plays an important role in achieving high electrochemical performance. The chemical information of solid electrolyte interphase (SEI) on Li metal after cycling was analyzed, as presented in Fig. 5c. The C 1s spectra after cycling can be deconvolved into three peaks at 284.1, 286.3, and 289 eV, which can be assigned to C-C, C-O/C≡N, and lithium carbonate. The C-O/C≡N peak can be attributed to PEO and SN decomposition at the Li surface. Three peaks at 397.1, 398.5, and 399.5 eV of N 1s spectra, can be assigned to the Li_3N, C═N–C, and C≡N bond. The formation of C═N-C and Li_3N indicates the polymerization of nitrile groups on the Li anode. The Li_3N content with a 4.4 V cutoff voltage is similar to those with a 4.2 V cutoff voltage. The S 2p spectra at 168.7 eV and 169.8 eV (doublet) indicate the presence of SO_2F species at the NMC surface, which is the result of $TFSI^-$ decomposition. F 1s shows two peaks at 684.6 eV and 688.4 eV. The LiF content with a 4.4 V cutoff voltage is higher than a 4.2 V cutoff voltage, as a result of decomposition of LiTFSI salt. The co-existence of mechanically stable LiF and ionically conductive Li_3N is beneficial to suppress side reactions between Li metal and SN [44]. To prove the high stability of PIPCE with cathode, NMC 811 is employed (Fig. S11). Initial charge and discharge capacity of NMC 811 is 161.3 and 127.4 mA h g^{-1}, corresponding to a CE of 79%. Discharge capacity increase to 175 mA h g^{-1} within 5 cycles, the number is 140 mA h g^{-1} after 30 cycles (~80% capacity retention).

The morphology of Li metal after 100 cycles under a cutoff voltage of

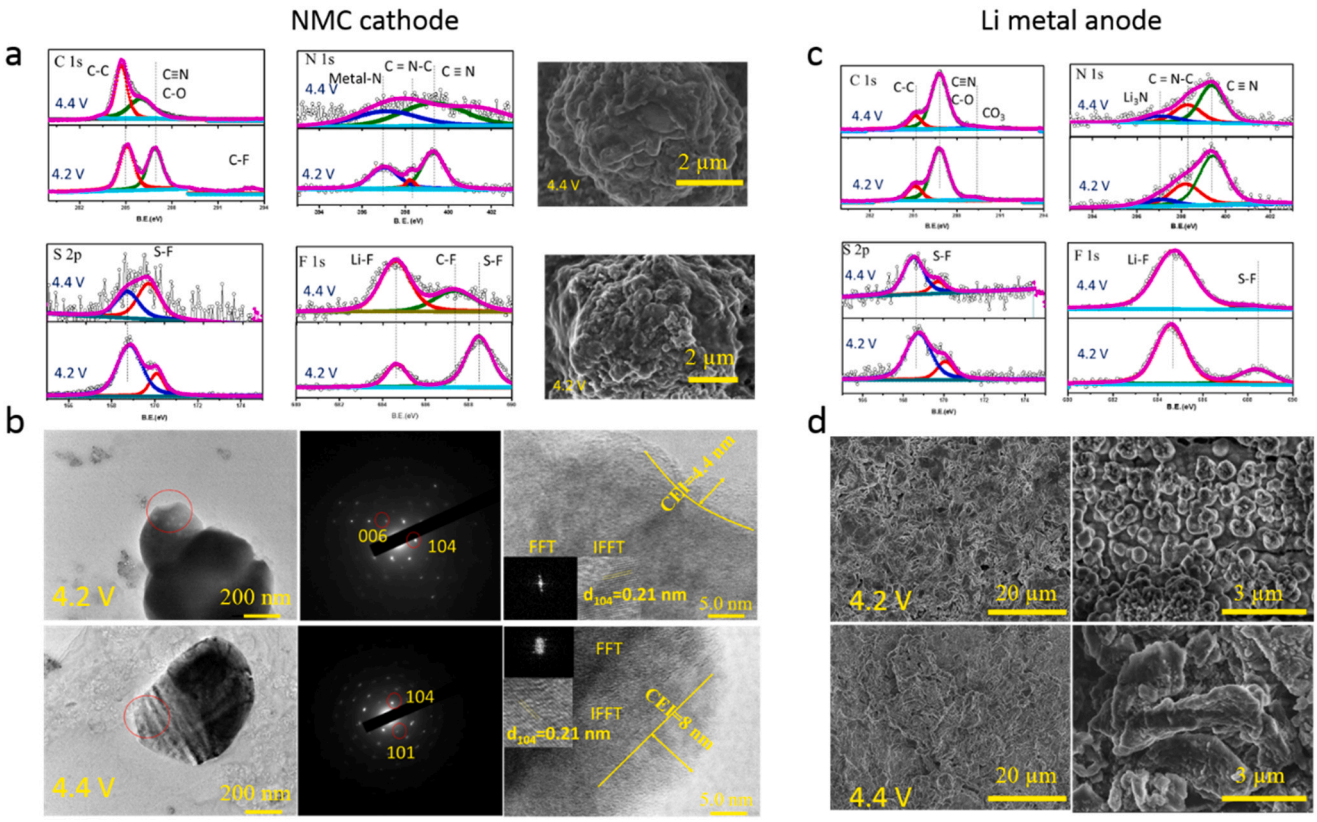

Fig. 5. XPS profiles of NMC 532 cathodes after cycling with a charge cutoff of 4.2 V (a) and 4.4 V (c). (b) TEM, SAED, and HRTEM images of NMC 532 cells with different cut-off voltages. (d) SEM images of Li metal with different cut-off voltages.

4.2 and 4.4 V was investigated by SEM. As shown in Fig. 5d, the surface of Li metal with a 4.2 V cutoff voltage shows a smoother morphology than the cell with a 4.4 V cutoff voltage. In the enlarged view, the deposited lithium at a cutoff voltage of 4.2 V shows a spherical morphology while a platelet Li deposition morphology is observed for deposition at a 4.4 V cutoff voltage. Additionally, the cross-section image of Li metal anode was recorded. As presented in Fig. S12, the corrosion layer on top of the Li metal anode is about 50 μm, close to PEO in quasi ionic liquid electrolyte [26]. To prove the high stability of PIPCE with anode, commercial Graphite is investigated (Fig. S13). First charge and discharge capacity of Graphite is 304.6 mA h g^{-1} and 382.8 mA h g^{-1}, corresponding to a first CE of 79.6%. Discharge capacity increase to 350 mA h g^{-1} in the following cycles, which proves that the PIPCE can be used for Graphite as well.

Based on the above analysis, we propose that the improved performance of PIPCE compared to pure PCE/PEO is due to the strong inter-molecular interactions (Fig. 6). The Li-ion is strongly bonded with SN, PEO, and TFSI ions. As a result, SN-LiTFSI offers the fast lithium ion transportation path while EO donates lone electron pair to Li cations. In addition, solvent-ion structure is tuned due to co-solvent effect of SN, FEC and PEO. SN reduction by Li metal and oxidation of PEO is suppressed because of interactions between PEO, SN and Lithium salt. FEC solvent addition is beneficial for the formation of F rich SEI and CEI component. SEI layer is composed of robust LiF and conductive Li_3N,

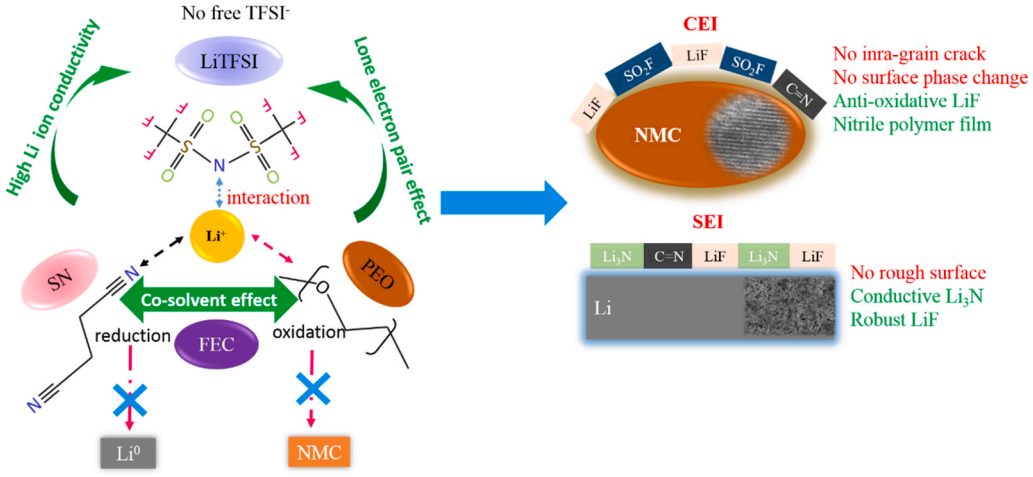

Fig. 6. Schematic of PIPCE electrolytes with inter-molecular interactions and stable interphase engineering at electrolyte/electrode interface.

which can stabilize the Li anode. At the cathode side, the CEI film is a mixed electronic/ionic conductor and nitrile polymer film can act as a buffer layer. Therefore, the oxidation of PEO by de-lithiated NMC is suppressed. As a result of stable SEI and CEI formed at the electrolyte/electrode interface, the Li/PIPCE/NMC cell is stable during long term cycling.

3. Conclusion

In this work, we developed a PIPCE strategy to widen the electrochemical window of PEO-based electrolytes for high-voltage Li metal batteries. Due to the intermolecular interactions, the oxidation voltage of 15% PEO PIPCE is increased to 4.97 V. The electrolyte demonstrates thermal stability as evidenced by thermal measurement and fire tests. Stable lithium plating/stripping performance of 700 h under a capacity of 1 mA h cm^{-2} is achieved. Full cells using NMC 532 as the cathode can deliver an initial capacity of 169 mA h g^{-1} and maintain a capacity retention of 80% after 100 cycles at a cutoff voltage of 4.4 V, which is far better than pure PEO and pure PCE electrolytes. Our result suggests that PIPCE is a promising direction for realizing high voltage Li metal batteries in the future.

CRediT authorship contribution statement

Yulong Liu: Conceptualization, Methodology, Experiment, Data analysis, Writing, Funding acquisition. **Yang Zhao:** Data curation, Writing - original draft, Writing - review & editing. **Wei Lu:** Data curation. **Liqun Sun:** Funding acquisition. **Lin Lin:** Data curation. **Matthew Zheng:** Writing - review & editing. **Xueliang Sun:** Data analysis, Writing - review & editing. **Haiming Xie:** Funding acquisition.

Declaration of Competing Interest

The authors declare that they have no known competing financial interests or personal relationships that could have appeared to influence the work reported in this paper.

Acknowledgements

This work was supported by National Key R&D Program of China (2016YFB0100500), Special Fund of Key Technology Research and Development Projects (20180201097GX, 20180201096GX, 20190302130GX), Jilin Province Science and Technology Department. The R&D Program of power batteries with low temperature and high energy, Science and Technology Bureau of Changchun (19SS013). Key Subject Construction of Physical Chemistry of Northeast Normal University. The Fundamental Research Funds for the Central Universities (2412019FZ015, 2412020QD006). Y. Zhao, M. Zheng and Prof. X. Sun thanks to the support from University of Western Ontario.

Appendix A. Supporting information

Supplementary data associated with this article can be found in the online version at doi:10.1016/j.nanoen.2021.106205.

References

[1] R. Chen, Q. Li, X. Yu, L. Chen, H. Li, Approaching practically accessible solid-state batteries: stability issues related to solid electrolytes and interfaces, Chem. Rev. 120 (2020) 6820–6877.
[2] H. Zhang, C. Li, M. Piszcz, E. Coya, T. Rojo, L.M. Rodriguez-Martinez, M. Armand, Z. Zhou, Single lithium-ion conducting solid polymer electrolytes: advances and perspectives, Chem. Soc. Rev. 46 (2017) 797–815.
[3] K. Zaghib, P. Charest, A. Guerfi, J. Shim, M. Perrier, K. Striebel, $LiFePO_4$ safe Li-ion polymer batteries for clean environment, J. Power Sources 146 (2005) 380–385.
[4] J. Liang, Y. Sun, Y. Zhao, Q. Sun, J. Luo, F. Zhao, X. Lin, X. Li, R. Li, L. Zhang, S. Lu, H. Huang, X. Sun, Engineering the conductive carbon/PEO interface to stabilize solid polymer electrolytes for all-solid-state high voltage $LiCoO_2$ batteries, J. Mater. Chem. A 8 (2020) 2769–2776.
[5] J. Liang, S. Hwang, S. Li, J. Luo, Y. Sun, Y. Zhao, Q. Sun, W. Li, M. Li, M.N. Banis, X. Li, R. Li, L. Zhang, S. Zhao, S. Lu, H. Huang, D. Su, X. Sun, Stabilizing and understanding the interface between nickel-rich cathode and PEO-based electrolyte by lithium niobium oxide coating for high-performance all-solid-state batteries, Nano Energy 78 (2020), 105107.
[6] Q. Li, T. Itoh, N. Imanishi, A. Hirano, Y. Takeda, O. Yamamoto, All solid lithium polymer batteries with a novel composite polymer electrolyte, Solid State Ion. 159 (2003) 97–109.
[7] K. Nie, X. Wang, J. Qiu, Y. Wang, Q. Yang, J. Xu, X. Yu, H. Li, X. Huang, L. Chen, Increasing poly(ethylene oxide) stability to 4.5 V by surface coating of the cathode, ACS Energy Lett. 5 (2020) 826–832.
[8] Q. Yang, J. Huang, Y. Li, Y. Wang, J. Qiu, J. Zhang, H. Yu, X. Yu, H. Li, L. Chen, Surface-protected $LiCoO_2$ with ultrathin solid oxide electrolyte film for high-voltage lithium ion batteries and lithium polymer batteries, J. Power Sources 388 (2018) 65–70.
[9] H. Miyashiro, Y. Kobayashi, S. Seki, Y. Mita, A. Usami, M. Nakayama, M. Wakihara, Fabrication of all-solid-state lithium polymer secondary batteries using Al_2O_3-coated $LiCoO_2$, Chem. Mater. 17 (2005) 5603–5605.
[10] J. Lu, J. Zhou, R. Chen, F. Fang, K. Nie, W. Qi, J.-N. Zhang, R. Yang, X. Yu, H. Li, L. Chen, X. Huang, 4.2 V poly(ethylene oxide)-based all-solid-state lithium batteries with superior cycle and safety performance, Energy Storage Mater. 32 (2020) 191–198.
[11] J. Lu, Z. Chen, F. Pan, Y. Cui, K. Amine, High-performance anode materials for rechargeable lithium-ion batteries, Electrochem. Energ. Rev. 1 (2018) 35–53.
[12] H.W. Tan, Y.M. Xu, D.D. Wu, A.T.Y. Lau, Recent insights into human bronchial proteomics – how are we progressing and what is next? Expert Rev. Proteom. 15 (2018) 113–130.
[13] C.F.N. Marchiori, R.P. Carvalho, M. Ebadi, D. Brandell, C.M. Araujo, Understanding the electrochemical stability window of polymer electrolytes in solid-state batteries from atomic-scale modeling: the role of li-ion salts, Chem. Mater. 32 (2020) 7237–7246.
[14] W. Zhou, S. Wang, Y. Li, S. Xin, A. Manthiram, J.B. Goodenough, Plating a dendrite-free lithium anode with a polymer/ceramic/polymer sandwich electrolyte, J. Am. Chem. Soc. 138 (2016) 9385–9388.
[15] X.-X. Zeng, Y.-X. Yin, N.-W. Li, W.-C. Du, Y.-G. Guo, L.-J. Wan, Reshaping lithium plating/stripping behavior via bifunctional polymer electrolyte for room-temperature solid li metal batteries, J. Am. Chem. Soc. 138 (2016) 15825–15828.
[16] C. Wang, T. Wang, L. Wang, Z. Hu, Z. Cui, J. Li, S. Dong, X. Zhou, G. Cui, Differentiated lithium salt design for multilayered PEO electrolyte enables a high-voltage solid-state lithium metal battery, Adv. Sci. 6 (2019), 1901036.
[17] B. Chen, Z. Huang, X. Chen, Y. Zhao, Q. Xu, P. Long, S. Chen, X. Xu, A new composite solid electrolyte PEO/$Li_{10}GeP_2S_{12}$/SN for all-solid-state lithium battery, Electrochim. Acta 210 (2016) 905–914.
[18] J.-H. Choi, C.-H. Lee, J.-H. Yu, C.-H. Doh, S.-M. Lee, Enhancement of ionic conductivity of composite membranes for all-solid-state lithium rechargeable batteries incorporating tetragonal $Li_7La_3Zr_2O_{12}$ into a polyethylene oxide matrix, J. Power Sources 274 (2015) 458–463.
[19] H. Huo, Y. Chen, J. Luo, X. Yang, X. Guo, X. Sun, Rational design of hierarchical "ceramic-in-polymer" and "polymer-in-ceramic" electrolytes for dendrite-free solid-state batteries, Adv. Energy Mater. 9 (2019), 1804004.
[20] D. Lin, W. Liu, Y. Liu, H.R. Lee, P.-C. Hsu, K. Liu, Y. Cui, High ionic conductivity of composite solid polymer electrolyte via in situ synthesis of monodispersed SiO_2 nanospheres in poly(ethylene oxide), Nano Lett. 16 (2016) 459–465.
[21] M. Chintapalli, T.N. Le, N.R. Venkatesan, N.G. Mackay, A.A. Rojas, J.L. Thelen, X. C. Chen, D. Devaux, N.P. Balsara, Structure and ionic conductivity of polystyrene-block-poly(ethylene oxide) electrolytes in the high salt concentration limit, Macromolecules 49 (2016) 1770–1780.
[22] T. Niitani, M. Shimada, K. Kawamura, K. Dokko, Y.-H. Rho, K. Kanamura, Synthesis of Li^+ ion conductive PEO-PSt block copolymer electrolyte with microphase separation structure, Electrochem. Solid-State Lett. 8 (2005) A385.
[23] J.A. Maslyn, L. Frenck, W.S. Loo, D.Y. Parkinson, N.P. Balsara, ACS Appl. Energy Mater. 2 (2019) 8197–8206.
[24] X. Pan, H. Sun, Z. Wang, H. Huang, Q. Chang, J. Li, J. Gao, S. Wang, H. Xu, Y. Li, W. Zhou, High voltage stable polyoxalate catholyte with cathode coating for all-solid-state Li-Metal/NMC622 batteries, Adv. Energy Mater. 10 (2020), 2002416.
[25] S. Qian, H. Chen, Z. Wu, D. Li, X. Liu, Y. Tang, S. Zhang, Designing ceramic/polymer composite as highly ionic conductive solid-state electrolytes, Batteries Supercaps 4 (2020) 39–59.
[26] H. Wu, Y. Xu, X. Ren, B. Liu, M.H. Engelhard, M.S. Ding, P.Z. El-Khoury, L. Zhang, Q. Li, K. Xu, C. Wang, J.G. Zhang, W. Xu, Polymer-in-"quasi-ionic liquid" electrolytes for high-voltage lithium metal batteries, Adv. Energy Mater. 9 (2019), 1902108.
[27] W. Zha, J. Li, W. Li, C. Sun, Z. Wen, Anchoring succinonitrile by solvent-Li+ associations for high-performance solid-state lithium battery, Chem. Eng. J. 406 (2021), 126754.
[28] K. Liu, Q. Zhang, B.P. Thapaliya, X.-G. Sun, F. Ding, X. Liu, J. Zhang, S. Dai, In situ polymerized succinonitrile-based solid polymer electrolytes for lithium ion batteries, Solid State Ion. 345 (2020), 115159.
[29] Q. Zhang, K. Liu, F. Ding, W. Li, X. Liu, J. Zhang, Safety-reinforced succinonitrile-based electrolyte with interfacial stability for high-performance lithium batteries, ACS Appl. Mater. Interfaces 9 (2017) 29820–29828.
[30] Z. Hu, F. Xian, Z. Guo, C. Lu, X. Du, X. Cheng, S. Zhang, S. Dong, G. Cui, L. Chen, Nonflammable nitrile deep eutectic electrolyte enables high-voltage lithium metal batteries, Chem. Mater. 32 (2020) 3405–3413.

[31] Y. Zhao, W.E. Tenhaeff, Thermally and oxidatively stable polymer electrolyte for lithium batteries enabled by phthalate plasticization, ACS Appl. Polym. Mater. 2 (2019) 80–90.
[32] L. Caradant, D. Lepage, P. Nicolle, A. Prébé, D. Aymé-Perrot, M. Dollé, Effect of Li + affinity on ionic conductivities in melt-blended nitrile rubber/polyether, ACS Appl. Polym. Mater. 2 (2020) 4943–4951.
[33] K. Kim, L. Kuhn, I.V. Alabugin, D.T. Hallinan, Lithium salt dissociation in diblock copolymer electrolyte using fourier transform infrared spectroscopy, Front. Energy Res. 8 (2020) 569442–569459.
[34] C. Wang, K.R. Adair, J. Liang, X. Li, Y. Sun, X. Li, J. Wang, Q. Sun, F. Zhao, X. Lin, R. Li, H. Huang, L. Zhang, R. Yang, S. Lu, X. Sun, Solid-state plastic crystal electrolytes: effective protection interlayers for sulfide-based all-solid-state lithium metal batteries, Adv. Funct. Mater. 29 (2019), 1900392.
[35] W. Liang, Y. Shao, Y.-M. Chen, Y. Zhu, ACS Appl. Energy Mater. 1 (2018) 6064–6071.
[36] G.B. Appetecchi, G.T. Kim, M. Montanino, F. Alessandrini, S. Passerini, Room temperature lithium polymer batteries based on ionic liquids, J. Power Sources 196 (2011) 6703–6709.
[37] J. Qiu, X. Liu, R. Chen, Q. Li, Y. Wang, P. Chen, L. Gan, S.J. Lee, D. Nordlund, Y. Liu, X. Yu, X. Bai, H. Li, L. Chen, Enabling stable cycling of 4.2 V high-voltage all-solid-state batteries with PEO-based solid electrolyte, Adv. Funct. Mater. 30 (2020), 1909392.
[38] S. Kaboli, H. Demers, A. Paolella, A. Darwiche, M. Dontigny, D. Clement, A. Guerfi, M.L. Trudeau, J.B. Goodenough, K. Zaghib, Behavior of solid electrolyte in Li-polymer battery with NMC cathode via in-situ scanning electron microscopy, Nano Lett. 20 (2020) 1607–1613.
[39] C. Fu, S. Lou, X. Xu, C. Cui, C. Li, P. Zuo, Y. Ma, G. Yin, Y. Gao, Capacity degradation mechanism and improvement actions for 4 V-class all-solid-state lithium-metal polymer batteries, Chem. Eng. J. 392 (2020), 123665.
[40] H. Chen, D. Adekoya, L. Hencz, J. Ma, S. Chen, C. Yan, H. Zhao, G. Cui, S. Zhang, Stable seamless interfaces and rapid ionic conductivity of Ca–CeO_2/LiTFSI/PEO composite electrolyte for high-rate and high-voltage all-solid-state battery, Adv. Energy Mater. 10 (2020), 2000049.
[41] Y. Lu, Y. Cai, Q. Zhang, L. Liu, Z. Niu, J. Chen, A compatible anode/succinonitrile-based electrolyte interface in all-solid-state Na-CO_2 batteries, Chem. Sci. 10 (2019) 4306–4312.
[42] S. Han, Y. Liu, H. Zhang, C. Fan, W. Fan, L. Yu, X. Du, Nitrogen removal of anaerobically digested swine wastewater by pilot-scale tidal flow constructed wetland based on in-situ biological regeneration of zeolite, Chemosphere 217 (2019) 364–373.
[43] Z. Li, H. Zhang, X. Sun, Y. Yang, Mitigating interfacial instability in polymer electrolyte-based solid-state lithium metal batteries with 4 V cathodes, ACS Energy Lett. 5 (2020) 3244–3253.
[44] A. Santiago, X. Judez, J. Castillo, I. Garbayo, A. Saenz de Buruaga, L. Qiao, G. Baraldi, J.A. Coca-Clemente, M. Armand, C. Li, H. Zhang, Improvement of lithium metal polymer batteries through a small dose of fluorinated salt, J. Phys. Chem. Lett. 11 (2020) 6133–6138.

Yulong Liu is currently associate professor at Northeast Normal University, China. Before working at Northeast Normal University, he was a postdoctoral fellow in Prof. Xueliang (Andy) Sun' Nanomaterials and Energy Group at the University of Western Ontario, Canada. He received his Bachelor degree from Central South University, China, in 2010, and Master degree in 2013. In 2018, he obtained his Ph.D. degree in Mechanical and Materials Engineering from University of Western Ontario. Previously, he worked together with GLABAT Solid State Battery Inc. on commercializing solid state batteries. His current research interests include nanomaterials for lithium ion batteries and high energy density solid-state batteries.

Dr. Yang Zhao is an Assistant Professor in the Department of Mechanical and Materials Engineering at the University of Western Ontario, Canada. Dr. Zhao received his B.S. and M.S. degrees from Northwestern Polytechnical University (Xi'an, China) in 2011 and 2014, respectively. He obtained his Ph.D. degree under the supervisor of Prof. Xueliang (Andy) Sun from the University of Western Ontario in 2018. Then, he had his postdoc training at Western and the Advanced Light Source of Lawrence Berkeley National Laboratory in 2019–2020. His research interests focus on advanced materials and interfaces for energy storage applications, and synchrotron-based X-ray techniques.

Wei Lu is a Ph.D. student of Department of Chemistry at the Northeast Normal University and National & Local United Engineering Laboratory for Power Battery. Her main research interests include Li metal anode for Li metal battery and conversion type anode material for Li ion battery.

Liqun Sun received her Ph.D. degree in physical chemistry from Northeast Normal University in 2012. Her current research interests focus on heat-resistant high safety separator for lithium ion batteries and high voltage all solid-state electrolytes for lithium metal batteries.

Lin Lin is a postgraduate Student of Department of Chemistry at the Northeast Normal University and National & Local United Engineering Laboratory for Power Battery. Her main research interests include Li metal anode for high-power Li metal battery.

Matthew Zheng is currently a Ph.D. student under the supervision of Xueliang (Andy) Sun at the University of Western Ontario, Canada. Matthew received his B.A.Sc. at the University of British Columbia in 2020. His research interests include application of 3D-printing and thin film coating techniques for lithium metal batteries.

Prof. Xueliang (Andy) Sun is a Canada Research Chair in Development of Nanomaterials for Clean Energy, Fellow of the Royal Society of Canada and Canadian Academy of Engineering and Full Professor at the University of Western Ontario, Canada. Dr. Sun received his Ph.D. in materials chemistry in 1999 from the University of Manchester, UK, which he followed up by working as a postdoctoral fellow at the University of British Columbia, Canada and as a Research Associate at L' Institut National de la Recherche Scientifique (INRS), Canada. His current research interests are focused on advanced materials for electrochemical energy storage and conversion.

Haiming Xie is a professor of Department of Chemistry at the Northeast Normal University and the director of National & Local United Engineering Laboratory for Power Battery. He received his Ph.D. degree from Northeast Normal University in 2008. His main research interests include lithium iron phosphate cathode materials and heat-resistant separators for high safety and high-power lithium ion batteries, low-temperature power batteries and all-solid-state electrolytes for lithium batteries.